Cell Death and Differentiation (2016) 23, 542–552

www.nature.com/cdd

c-Abl–p38α signaling plays an important role in MPTP-induced neuronal death

R Wu[1,2], H Chen[1,3], J Ma[1,2], Q He[1,2], Q Huang[4], Q Liu[5], M Li*[,4] and Z Yuan*[,1,2,3]

Oxidative stress is a major cause of sporadic Parkinson's disease (PD). Here, we demonstrated that c-Abl plays an important role in oxidative stress-induced neuronal cell death. C-Abl, a nonreceptor tyrosine kinase, was activated in an 1-methyl-4-phenyl-1,2,3,6-tetrahydropyridine hydrochloride (MPTP)-induced acute PD model. Conditional knockout of c-Abl in neurons or treatment of mice with STI571, a c-Abl family kinase inhibitor, reduced the loss of dopaminergic neurons and ameliorated the locomotive defects induced by short-term MPTP treatment. By combining the SILAC (stable isotope labeling with amino acids in cell culture) technique with other biochemical methods, we identified p38α as a major substrate of c-Abl both *in vitro* and *in vivo* and c-Abl-mediated phosphorylation is critical for the dimerization of p38α. Furthermore, p38α inhibition mitigated the MPTP-induced loss of dopaminergic neurons. Taken together, these data suggested that c-Abl–p38α signaling may represent a therapeutic target for PD.
Cell Death and Differentiation (2016) **23,** 542–552; doi:10.1038/cdd.2015.135; published online 30 October 2015

Parkinson's disease (PD), the second most common neurodegenerative disorder, is characterized by bradykinesia, rigidity, tremor, and loss of dopaminergic neurons.[1] Familial mutations that cause PD have been identified, including in the genes that encode α-synuclein and leucine-rich repeat kinase 2 (LRRK2) that cause autosomal-dominant PD, and DJ-1, PINK1, and parkin that cause autosomal-recessive PD.[2] However, the majority of PD cases are sporadic. The cause of sporadic PD remains unknown, and the role of environmental toxins and genetic factors in sporadic PD is unclear. However, the evidence regarding postencephalitic PD and the discovery of 1-methyl-4-phenyl-1,2,3,6-tetrahydropyridine hydrochloride (MPTP)-induced Parkinsonism suggest that environmental toxins may be a major cause of sporadic PD.[3,4]

The neurotoxins used to induce dopaminergic neurodegeneration, including 6-hydroxydopamine, MPTP, and rotenone, induce the formation of reactive oxygen species (ROS). ROS react with nucleic acids, proteins, and lipids to induce mitochondrial damage. Although oxidative stress plays a critical role in causing PD, the mechanisms underlying oxidative stress-induced PD remain unclear.

The nonreceptor tyrosine kinase c-Abl is ubiquitously expressed and mediates a variety of extrinsic and intrinsic cell signaling activities, including growth factor signaling, cell adhesion, oxidative stress, and DNA damage.[5] Our group and other groups have reported that c-Abl plays an important role in oxidative stress-induced neuronal death.[6–8] Recently, Ko *et al.*[9] and Imam *et al.*[10] have reported that c-Abl phosphorylated Parkin and inhibited its E3 ligase activity that led to the neurotoxic accumulation of Parkin's substrates. α-Synuclein has also been reported to be substrates of c-Abl and to participate in PD pathogenesis.[9–11] The c-Abl inhibitor Nilotinib and INNO-406 have been reported prevents the loss of dopamine neurons and improves motor behavior in a murine PD model.[12–14]

In this study, we demonstrated that c-Abl is activated in oxidative stress-induced PD. Both the conditional knockout (KO) of c-Abl and treatment with the c-Abl inhibitor STI571 protect against MPTP-induced PD. Using the SILAC (stable isotope labeling with amino acids in cell culture) technique, we showed that p38α is a novel c-Abl substrate that mediates oxidative stress-induced PD. The phosphorylation of p38α at Y182 and Y323 by c-Abl promotes p38α dimerization, thereby activating p38α via a noncanonical pathway. The inhibition of p38α using SB203580 mitigates the MPTP-induced loss of dopaminergic neurons. Taken together, we found that c-Abl–p38α signaling plays a role in oxidative stress-induced PD.

[1]State Key Laboratory of Brain and Cognitive Sciences, Institute of Biophysics, Chinese Academy of Sciences, Beijing 100101, China; [2]College of Life Sciences, University of Chinese Academy of Sciences, Beijing 100049, China; [3]Center of Alzheimer's Disease, Beijing Institute for Brain Disorders, Beijing 100069, China; [4]Department of Pharmacology and the Proteomics Center, Zhongshan School of Medicine, Sun Yat-sen University, Guangzhou 510080, China and [5]High Magnetic Field Laboratory, Chinese Academy of Sciences, Hefei, Anhui 230031, China

*Corresponding author: M Li, Department of Pharmacology and the Proteomics Center, Zhongshan School of Medicine, Sun Yat-sen University, Guangzhou 510080, China. Tel: +86 20 87331553; Fax: +86 20 87331653; E-mail: limt@mail.sysu.edu.cn

or Z Yuan, State Key Laboratory of Brain and Cognitive Sciences, Institute of Biophysics, Chinese Academy of Sciences, Beijing 100101, China. Tel: +86 10 64867137; Fax: +86 10 64867137; E-mail: zqyuan@ibp.ac.cn

Abbreviations: AIMP2, aminoacyl tRNA synthetase complex-interacting multifunctional protein 2; ANOVA, one-way analysis of variance; DAB, 3,3′-diaminobenzidine; EGTA, ethylene glycol tetraacetic acid; FAK, focal adhesion kinase; FBP1, far upstream element-binding protein 1; FBS, fetal bovine serum; GST, glutathione *S*-transferase; HPLC, high-performance liquid chromatography; HRP, horseradish peroxidase; IP, immunoprecipitation; JNK, c-Jun N-terminal kinase; KD, kinase dead; KO, knockout; LC-MS, liquid chromatography–mass spectrometry; LRRK2, leucine-rich repeat kinase 2; MAPK, mitogen-activated protein kinase; MPP^+, 1-methyl-4-phenylpyridinium; MPTP, 1-methyl-4-phenyl-1,2,3,6-tetrahydropyridine hydrochloride; MST1, mammalian Ste20-like kinase 1; PD, Parkinson's disease; PINK1, PTEN-induced putative kinase 1; ROS, reactive oxygen species; SILAC, stable isotope labeling with amino acids in cell culture; TBST, Tris-buffered saline and Tween-20; TFA, trifluoroacetate; TH, tyrosine hydroxylase; TSA, tyramide signal amplification; WASP, Wiskott–Aldrich syndrome protein; WT, wild type

Received 15.4.15; revised 30.8.15; accepted 07.9.15; Edited by R Knight; published online 30.10.15

Results

Conditional KO of c-Abl in neurons protects against MPTP-induced death of dopaminergic neurons. We previously reported that c-Abl mediates oxidative stress-induced neuronal death.[6,7] Here, we investigated the role of c-Abl in oxidative stress-induced neurodegeneration and the underlying mechanisms. C57BL/6J mice were used to assess the importance of c-Abl in the MPTP-induced model of PD. The mice were treated with either saline or MPTP (four intraperitoneal injections of 20 mg/kg at 2 h intervals). At 2 h and on each of 7 consecutive days after the final MPTP injection, c-Abl phosphorylation at Y245 was measured in the striatum to determine the level of c-Abl activation. MPTP treatment caused a 1.4-fold increase in the phospho-Y245-c-Abl level from 2 h to 2 days after MPTP injection. We observed a dramatic decrease in the tyrosine hydroxylase (TH) protein levels 1 day after MPTP injection, followed by a mild decrease in TH expression from 3 to 7 days after MPTP injection (Figures 1a and b). These data suggested that c-Abl activation may participate in the MPTP-induced loss of dopaminergic neurons. To confirm this result, c-Abl$^{flox/flox}$ mice were crossed with CaMKII-iCre transgenic mice to generate conditional KO of c-Abl in neurons. Wild-type (WT, c-Abl$^{flox/flox}$) and c-Abl KO (c-Abl$^{flox/flox}$; CaMKII-iCre$^{+/-}$) mice were treated with saline or MPTP (four intraperitoneal injections of 20 mg/kg at 2 h intervals). After treatment with MPTP, the loss of neurons was monitored via stereological analysis of TH or Nissl immunostaining in substantia nigra. MPTP induced the loss of ~40% of the TH-positive neurons (Figures 1c and d) and the similar result was observed in Nissl staining (Figure 1e). The neuron-specific KO of c-Abl resulted in significant protection against the MPTP-induced death of neurons compared with endogenous WT c-Abl expression (Figures 1c–e). The level of the TH protein in the striatum also indicated that c-Abl KO prevented the loss of dopaminergic neurons following MPTP exposure (Figures 1f and g).

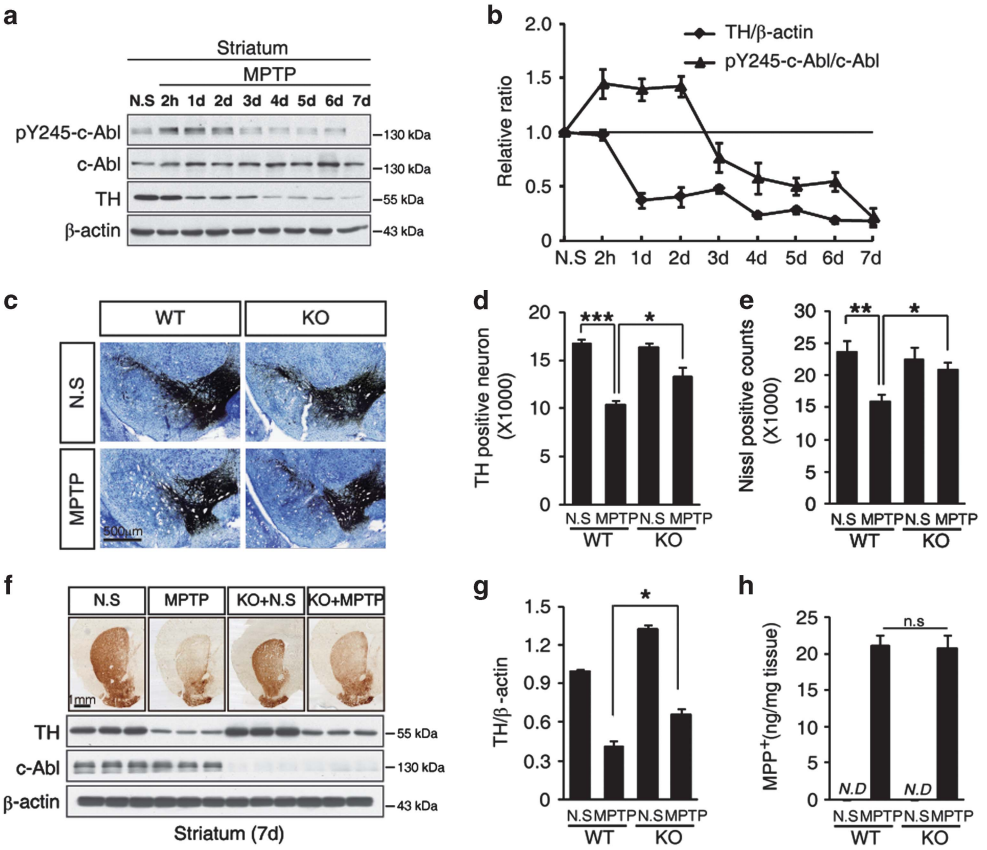

Figure 1 c-Abl is activated in an MPTP-induced PD model. (**a**) C57BL/6J mice were treated with saline or MPTP (four i.p. injections of 20 mg/kg at 2 h intervals). Striatum tissue was collected at 2 h and on each of 7 consecutive days after MPTP injection. The striatal tissue lysates were immunoblotted using an anti-phospho-Y245-c-Abl (pY245-c-Abl) antibody to determine the levels of tyrosine-phosphorylated c-Abl. An anti-β-actin antibody was used as a loading control, and a anti-TH antibody was used to label dopaminergic neurons after MPTP treatment. (**b**) The normalized levels of pY245-c-Abl and TH. The data are expressed as mean ± S.E.M. (**c**) Photomicrographs of TH and Nissl co-stained sections from the substantia nigra of WT and c-Abl KO littermate mice treated with saline or MPTP. (**d** and **e**) The number of TH-positive neurons (**d**) and Nissl-stained cells (**e**) in the substantia nigra of the WT and c-Abl KO littermate mice treated with saline or MPTP, as determined by stereological quantification. The data are expressed as mean ± S.E.M. (ANOVA, $^*P<0.05$, $^{**}P<0.01$, $^{***}P<0.001$, $n=5$). (**f**) Photomicrographs of TH-immunostained sections from the striatum of WT and c-Abl KO littermate mice treated with saline or MPTP (upper panel). Striatal tissue was collected from WT and c-Abl KO littermate mice 7 days after treatment with saline or MPTP and was subjected to immunoblotting using the indicated antibodies (bottom panel). (**g**) The normalized levels of TH based on quantification using ImageJ software (NIH). The data are expressed as mean ± S.E.M. (ANOVA, $^*P<0.05$, $n=3$). (**h**) Levels of MPP^+ in the striatum of WT and c-Abl KO mice treated with saline and MPTP (four i.p. injections. 20 mg/kg, at 2 h intervals). ND, not detected

In addition, we observed that there is similar concentration of MPP^+, the active metabolite of MPTP in the brain, in WT and c-Abl KO mice (Figure 1h). Together, these data suggested that MPTP mediates the activation of c-Abl and that the neuron-specific KO of c-Abl prevents MPTP-induced dopaminergic neuronal death.

STI571 reduces the loss of dopaminergic neurons and ameliorates the locomotive defects induced by acute MPTP treatment. To determine whether an inhibitor of c-Abl protects against the MPTP-induced loss of dopaminergic neurons, we treated animals with STI571, a c-Abl family kinase inhibitor, before or after exposure to MPTP (Figure 2a). It has been shown that intraperitoneally injected STI571 could penetrate into brain,[15] and we confirmed the presence of STI571 in the ventral midbrain by intraperitoneal injection in our experiments (Figure 2b). Moreover, we found that intraperitoneal injection of STI571 did not affect the concentration of MPP^+, the metabolite of MPTP, in the striatum (Figure 2c). Pretreating mice with STI571 prevented the MPTP-induced tyrosine phosphorylation of c-Abl (Figure 2d). At 7 days after the final MPTP injection, stereological analysis of the TH-positive neurons and Nissl staining cell showed that STI571 markedly protected against the MPTP-induced death of neurons (Figures 2e–g). The expression levels of TH in the striatum were dramatically decreased following MPTP treatment, but STI571 treatment significantly rescued the level of TH (Figures 2h and i). The loss of dopaminergic neurons from the substantia nigra is always accompanied by the development of motor defects. Rota-Rod tests showed that STI571 protected against MPTP-induced locomotive defects (Figure 2j). These data showed that treatment with an inhibitor of c-Abl rescues dopaminergic neurons from MPTP-induced death. Therefore, treatment with a c-Abl inhibitor may also improve motor defects in patients with PD.

SILAC identified p38α as the major substrate for c-Abl during oxidative stress. It has been reported that c-Abl mediates PD pathogenesis via targets such as parkin and α-synuclein.[9,10,16] However, the molecular mechanisms by which c-Abl participates in oxidative stress-induced PD remain unknown. Because c-Abl is a tyrosine kinase, its substrates can be determined via SILAC technology followed by the identification of the tyrosine-phosphorylated peptides. Three populations of SH-SY5Y cells were independently cultured in the presence of 'light' arginine (Arg0 $^{12}C_6^{14}N_4$) and lysine (Lys0 $^{12}C_6^{14}N_2$), 'medium' arginine (Arg6 $^{13}C_6^{14}N_4$) and lysine (Lys6 $^{13}C_6^{14}N_2$), or 'heavy' arginine (Arg10 $^{13}C_6^{15}N_4$) and lysine (Lys8 $^{13}C_6^{15}N_2$) (Figure 3a). The labeled SH-SY5Y cells were treated with vehicle, hydrogen peroxide alone, or hydrogen peroxide and the c-Abl inhibitor STI571. Partial cell lysates were immunoprecipitated using an anti-pan-phosphotyrosine antibody and then immunoblotted using an anti-c-Abl antibody. Hydrogen peroxide treatment induced c-Abl activation (Figure 3b). The labeled cells were lysed under denaturing conditions and were mixed together in equal portions. The tyrosine-phosphorylated peptides were isolated and analyzed via liquid chromatography–mass spectrometry (LC-MS).

In the list of possible substrates of c-Abl by SILAC, Arg,[17] focal adhesion kinase (FAK),[18] Caveolin-1,[19] and Wiskott–Aldrich syndrome protein (WASP)[20] have been reported. Interestingly, a subgroup of mitogen-activated protein kinases (MAPKs) were identified in the peptide list (Figure 3c), among which MAPK14 (encoding p38α) expression was increased 3.6-fold by hydrogen peroxide treatment and was decreased by ~30% by STI571 treatment. These data suggested that p38α may serve as a substrate of the kinase c-Abl under oxidative stress conditions. To confirm that p38α is a substrate of c-Abl, the SILAC samples were immunoprecipitated using an anti-pan-phosphotyrosine antibody and were immunoblotted using an anti-p38α antibody. The increased tyrosine phosphorylation of p38α mediated by oxidative stress was mitigated by STI571 (Figure 3d). Accordingly, *in vitro* kinase assays demonstrated that the kinase c-Abl phosphorylated p38α (Figure 3e). Moreover, the c-Abl-mediated phosphorylation of p38α was observed using WT c-Abl but not kinase-dead (KD) c-Abl (Figure 3f).

c-Abl interacts with p38α and phosphorylates p38α at Y182 and Y323. To determine whether p38α directly interacts with c-Abl, a glutathione *S*-transferase (GST) pull-down assay was performed by incubating the recombinant GST-p38α with cell lysates that expressed Myc-tagged c-Abl. C-Abl interacts with GST–p38α but not GST alone (Figure 4a). Co-immunoprecipitation results showed that c-Abl interacts with p38α in cells (Figures 4b and c). To further map the p38α phosphorylation sites targeted by c-Abl kinase, *in vitro* phosphorylated p38α was subjected to mass spectrometry analysis. Phosphorylated tyrosine was identified at two sites, tyrosine 182 (Y182) and tyrosine 323 (Y323) (Figure 4d). In cell culture experiments, c-Abl phosphorylated p38α-WT; however, the phosphorylation of p38α-Y182F, p38α-Y323F, and p38α-Y182F/Y323F by c-Abl was dramatically reduced (Figure 4e). These data suggested that c-Abl phosphorylates p38α at Y182 and Y323. Consistently, we observed p38α autophosphorylation (T180/Y182), and STI571 treatment inhibits this phosphorylation (Figure 3d). Interestingly, the autophosphorylation of p38α at T180/Y182 was decreased when Y323 was replaced with a phenylalanine (Figure 4e). In addition to the well-characterized activation of p38α via phosphorylation at both residues of the p38α TxY activation loop motif by dual T/Y-specific MAPK kinases, p38α is activated via a noncanonical pathway via homodimerization.[21] These data suggested that c-Abl mediates p38α activation via both canonical (Y182) and noncanonical (Y323) pathways.

To further explore the molecular mechanisms regulating the phosphorylation of p38α at Y323 by the kinase c-Abl, we expressed EGFP-tagged p38α and FLAG-tagged p38α in cells to examine p38α homodimerization. The coexpression of p38α and c-Abl dramatically increased the homodimerization of WT p38α but not Y323F mutant p38α (Figure 4f). These data indicated that p38α phosphorylation at Y323 by c-Abl promotes p38α homodimerization and activates p38α via a noncanonical pathway.

C-Abl mediates p38α activation in PD model. The finding that c-Abl phosphorylates p38α led us to investigate the role

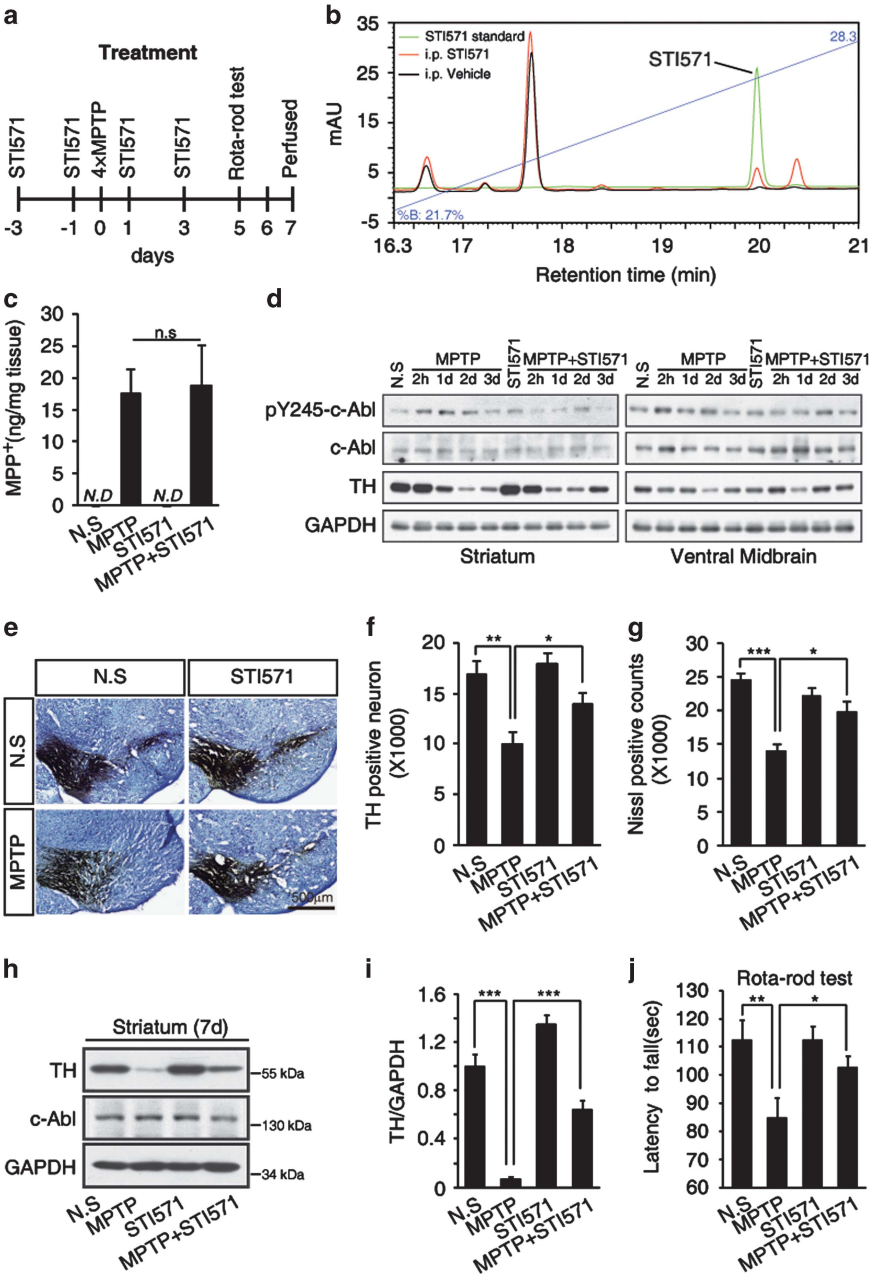

Figure 2 The c-Abl inhibitor STI571 reduces dopaminergic neuronal cell death and locomotive defects induced by acute MPTP treatment. (**a**) Experimental design. For drug treatment, the C57BL/6J mice were treated with STI571 (four i.p. injections of 30 mg/kg at 1-day intervals) followed by an additional injection 12 h after treatment with MPTP (four i.p. injections of 20 mg/kg at 2 h intervals). The mice were killed 7 days after the final MPTP injection. Behavior was assessed using the Rota-Rod test 5 days after the final MPTP injection. (**b**) Brain penetration of STI571 in ventral midbrain 2 h after intraperitoneal injection. (**c**) Mice were treated as in (**a**) and killed 90 min after final MPTP injection. The levels of MPP^+ in the striatum of the mice were measured by HPLC analysis. (**d**) C57BL/6J mice were treated with STI571 (i.p. injections of 30 mg/kg at 1-day intervals) and MPTP as shown in (**a**). Tissue was collected from the striatum and ventral midbrain at indicated time points after the final MPTP injection and was subjected to immunoblotting using an anti-pY245-c-Abl antibody to determine the level of activated c-Abl. An anti-GAPDH antibody was used as a loading control. (**e**) Photomicrographs of TH and Nissl co-stained sections in the substantia nigra of mice treated as in (**a**). (**f** and **g**) The number of TH-positive neurons (**f**) and Nissl-stained cells (**g**) as determined by stereological quantification in the substantia nigra of mice treated as in (**a**). Data are expressed as mean ± S.E.M. (ANOVA, $^*P<0.05$, $^{**}P<0.01$, $n=5$). (**h**) C57BL/6J mice were treated as in (**a**), and tissue was collected from the striatum. The striatal tissue lysates were immunoblotted using an anti-TH antibody to examine the loss of dopaminergic neurons. (**i**) The normalized levels of TH. The data are expressed as mean ± S.E.M. (ANOVA, $^{***}P<0.001$, $n=3$). (**j**) The latency of the mice on the Rota-Rod. The data are expressed as mean ± S.E.M. (ANOVA, $^*P<0.05$, $^{**}P<0.01$, $n=12$ per group)

of c-Abl–p38α signaling in neurodegenerative disease models. First, treatment with 1-methyl-4-phenylpyridinium (MPP^+, the active metabolite of MPTP) increased p38α phosphorylation in SH-SY5Y cells, and this phosphorylation was mitigated by c-Abl inhibition (Figure 5a). In an acute mouse model of PD, we observed that the level of p38α phosphorylated at T180/Y182 in the ventral midbrain was increased following treatment with MPTP and mitigated by

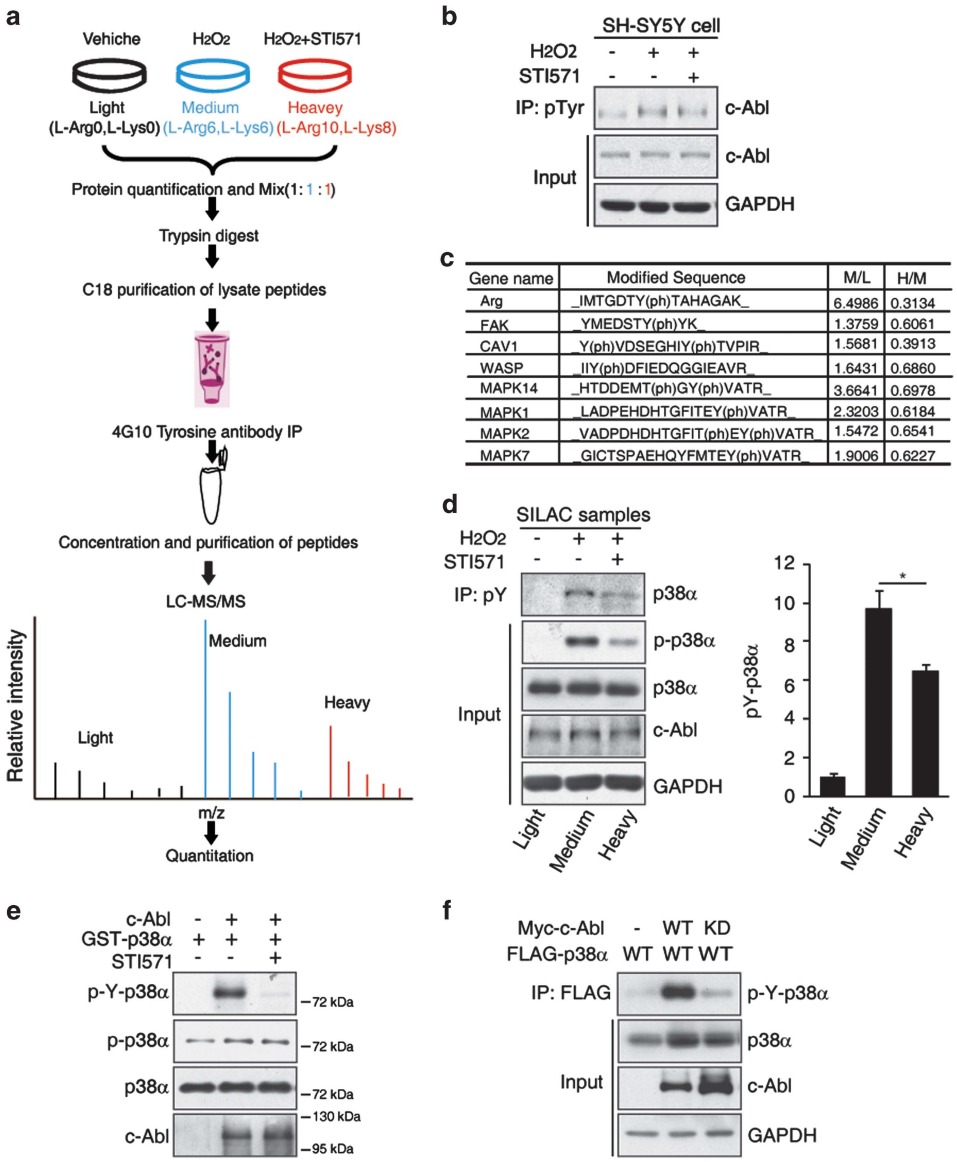

Figure 3 SILAC identifies p38α as a major substrate of c-Abl during oxidative stress. (**a**) The experimental design in which SILAC was performed to screen for c-Abl substrates under conditions of oxidative stress. Briefly, three populations of SH-SY5Y cells were metabolically labeled with normal arginine and lysine (Arg0 and Lys0), or forms that are 6 (Arg6 and Lys6) or 10/8 Daltons heavier (Arg10 and Lys8). After treatment with H_2O_2 with or without STI571, the cell lysates were quantified and mixed together in equal portions. After digestion with trypsin, the lysates were immunoprecipitated using antibodies against phosphotyrosine. The precipitated peptides were analyzed via LC-MS. (**b**) The SILAC-labeled SH-SY5Y cells were untreated or treated with 800 μM H_2O_2 for 30 min in the presence or absence of 5 μM STI571. The cell lysates were immunoprecipitated using an anti-phosphotyrosine antibody followed by immunoblotting using an antibody against c-Abl. (**c**) The list of identified proteins by SILAC. (**d**) The SH-SY5Y cell lysates used for SILAC were subjected to immunoprecipitation using an anti-phosphotyrosine antibody and immunoblotting using antibodies against p38α, phospho-p38α (T180/Y182), c-Abl, and GAPDH. The bar graph in the right panel shows the quantification of p38α tyrosine phosphorylation (ANOVA, $^*P<0.05$, $n=3$). (**e**) Kinase-active c-Abl was untreated or treated with 5 μM STI571 and then subjected to an *in vitro* kinase assay using full-length GST-p38α as a substrate. The phosphorylation reactions were analyzed via immunoblotting using anti-phosphotyrosine and anti-phospho-p38α (T180/Y182, p-p38α) antibodies. p38α was tyrosine phosphorylated by c-Abl and was autophosphorylated at T180 *in vitro*. (**f**) Lysates of 293T cells transfected with FLAG-tagged p38α alone or together with Myc-tagged c-Abl-WT or c-Abl-KD (kinase-dead) expression plasmids were immunoprecipitated using an anti-FLAG antibody and were analyzed via immunoblotting using an anti-phosphotyrosine antibody. p38α was tyrosine phosphorylated by c-Abl kinase *in vivo*

treatment with STI571 (Figure 5b). Accordingly, phosphorylation of p38α in the striatum was also dramatically increased following treatment with MPTP, peaking after 3 days (Figures 5c and d). Furthermore, we found that p38 phosphorylation sustains in the MPTP model even after c-Abl phosphorylation levels returns to the baseline, indicating that c-Abl is an upstream kinase of p38 under oxidative stress.

To confirm that c-Abl mediates p38α phosphorylation *in vivo*, c-Abl$^{flox/flox}$ mice were crossed with CaMKIIα-iCre transgenic mice that generate a conditional KO of c-Abl in neurons.[22] The age-matched WT and c-Abl KO littermates were treated with

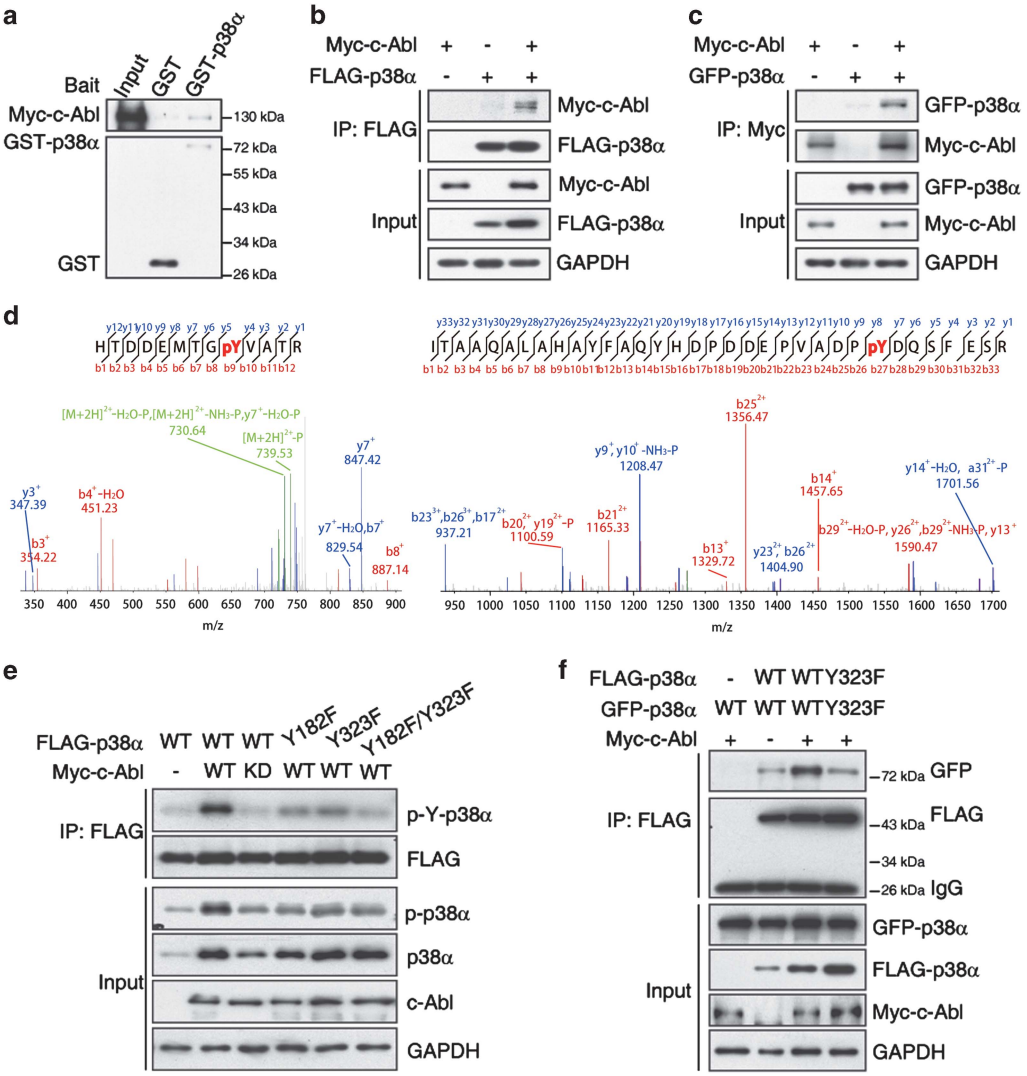

Figure 4 c-Abl interacts with p38α and phosphorylates p38α at Y182 and Y323. (**a**) 293T cells were transfected with Myc-tagged c-Abl and cell lysates were incubated with GST-p38α or GST protein and Glutathione-Sepharose beads followed by immunoblotting with anti-Myc antibody. (**b**) Lysates from 293T cells transfected with indicated plasmids were subjected to immunoprecipitation with anti-FLAG antibody, followed by immunoblotting with anti-Myc or anti-FLAG antibody. (**c**) Lysates from 293T cells transfected indicated plasmids were subjected to immunoprecipitation with anti-Myc antibody, followed by immunoblotting with anti-GFP or anti-Myc antibody. (**d**) The phosphorylation reactions from Figure 3e were subjected to SDS-PAGE followed by Coomassie Blue staining. The band corresponding to p38α was excised from the gel and digested with trypsin. The phosphorylation sites were mapped via microcapillary LC-MS/MS, resulting in 77.8% coverage of the p38α amino acid sequence. Two phosphopeptides consistent with p38α phosphorylation at Y182 and Y323 were identified. (**e**) Lysates of 293T cells transfected with FLAG-tagged WT, Y182F, Y323F or Y182F, and Y323F p38α alone or together with Myc-tagged c-Abl-WT or c-Abl-KD expression plasmids were immunoprecipitated using an anti-FLAG antibody and were analyzed via immunoblotting using anti-phosphotyrosine and anti-FLAG antibodies. Y182 and Y323 are sites of p38α that are phosphorylated by c-Abl. (**f**) Lysates of 293T cells transfected with GFP-tagged WT or Y323F p38α alone or with Myc-tagged c-Abl and FLAG-tagged WT or Y32F p38α expression plasmids were immunoprecipitated using an anti-FLAG antibody and were analyzed via immunoblotting using anti-GFP and anti-FLAG antibodies. The c-Abl-mediated phosphorylation of p38α at Y323 promotes p38α dimerization

saline or MPTP (four intraperitoneal injections of 20 mg/kg at 2 h intervals) and killed 40 h after the final MPTP injection. Immunohistochemistry results show that c-Abl KO abrogated the increase in the levels of phospho-p38*α* in the TH-positive neurons and neuritic terminals of TH-positive neurons in the striatum (Figure 5e). It has been reported that acute MPTP treatment will induce microglial activation by MPP^+ or agents released by injured neurons.[23] Accordingly, we also found that the level of phosphorylated p38*α* increased in microglial cells (Figure 5e), Interestingly, less microglial activation in the striatum of neuron-specific c-Abl KO mice was observed, and this might be due to reduced damaged neurons in c-Abl KO brain (Figure 5e). Furthermore, immunoblotting showed that there was a significant decreased level of phosphorylated p38*α* in both ventral midbrain and striatum from c-Abl KO mice compared with WT mice upon MPTP treatment (Figure 5f). Taken together, these data suggested that c-Abl endogenously phosphorylates p38*α* and promotes neuronal cell death.

The p38*α* inhibition alleviates MPTP-induced dopaminergic neuron loss and motor defects. After establishing the role of c-Abl–p38*α* signaling in MPTP-induced dopaminergic

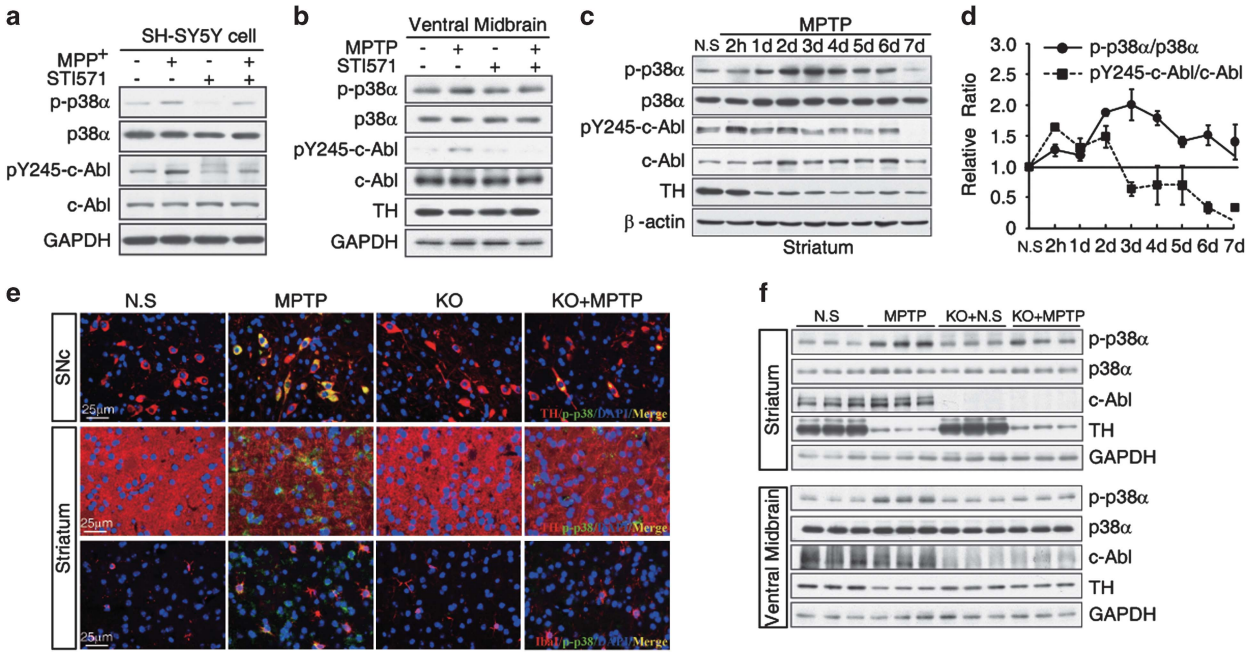

Figure 5 C-Abl mediated p38α activation in the PD model. (**a**) SH-SY5Y cells were untreated or treated with 1 mM MPP^+ for 1 h in the presence or absence of 5 μM STI571. The cell lysates were immunoblotted using an anti-phospho-p38α (Thr180/Y182, p-p38α) antibody. (**b**) C57BL/6 J mice were treated with STI571 (two i.p. injections of 30 mg/kg at 1-day intervals) before MPTP treatment as in Figure 2a. Tissue was collected from ventral midbrain at 2 h after the final MPTP injection and subjected to immunoblotting with anti-phospho-p38α (Thr180/Y182, p-p38α) antibody or anti-pY245-c-Abl antibody. An anti-GAPDH antibody was used as a loading control. (**c**) C57BL/6J mice were treated with saline or MPTP (four i.p. injections of 20 mg/kg at 2 h intervals), and striatal tissue was collected at 2 h and on each of 7 consecutive days after MPTP treatment. The striatal tissue lysates were immunoblotted using an anti-phospho-p38α (Thr180/Y182, p-p38α) antibody to detect the level of activated p38α, using anti-phospho-Y245-c-Abl (pY245-c-Abl) to detect tyrosine-phosphorylated c-Abl, using an anti-actin antibody as a loading control, and using a TH antibody to detect the number of surviving dopaminergic neurons after MPTP treatment. (**d**) The normalized levels of p-p38α and pY245-c-Abl. The data are expressed as mean ± S.E.M. (**e**) Immunofluorescence images of TH/Iba1 (red), phospho-p38α (green), and merged staining (yellow) in substantia nigra or striatum from MPTP-treated c-Abl KO mice or WT littermates. (**f**) Lysates of striatum or ventral midbrain from WT and c-Abl KO littermate mice after treatment with saline or MPTP were immunoblotted with anti-phospho-p38α (Thr180/Y182, p-p38α) antibody

neuronal death, we further examined whether p38α inhibition might provide therapeutic value for oxidative stress-induced PD mice. C57BL/6J mice were treated with either saline or MPTP (four intraperitoneal injections of 20 mg/kg at 2 h intervals) with or without the p38α-specific inhibitor SB203580 (Figure 6a). We first confirmed brain penetration of intraperitoneally injected SB203580 in the ventral midbrain by high-performance liquid chromatography (HPLC) analysis (Figure 6b), and we also found that intraperitoneal injection of SB203580 did not affect the concentration of MPP^+ in the striatum (Figure 6c). Interestingly, SB20580 treatment abolished MPTP-induced p38α phosphorylation in both TH-positive neurons from substantia nigra and neuritic terminals of TH-positive neurons in the striatum (Figure 6d). Moreover, the inhibition of p38α markedly prevented the MPTP-induced loss of TH-positive neurons or Nissl-stained cells in the substantia nigra (Figures 6e–g). In addition, MPTP-induced down-regulation of TH expression in the striatum could be rescued by p38α inhibitor (Figures 6h and i). Rota-Rod assays showed that SB203580 treatment significantly improved the motor activity of the MPTP-treated PD mice (Figure 6j). Taken together, these data indicated that p38α inhibition may represent a strategy for treating oxidative stress-induced PD.

Discussion

The major finding of this study is that c-Abl mediates the activation of p38α in mice with MPTP-induced PD. First, c-Abl was activated following treatment with MPTP. The conditional KO of c-Abl in neurons or treatment with a c-Abl inhibitor rescued the MPTP-induced loss of dopaminergic neurons. Second, based on SILAC analysis, we identified p38α as a novel direct target of c-Abl. We also confirmed that c-Abl phosphorylates p38α and activates p38α by increasing p38α dimerization. Finally, we showed that inhibiting p38α rescues dopaminergic neurons from MPTP-induced death, suggesting that treatment with an inhibitor of c-Abl or p38α may serve as an effective therapy for PD.

The nonreceptor tyrosine kinase c-Abl is activated by cellular stress[24] and plays a critical role in chronic myeloid leukemia that has been commonly treated with the c-Abl inhibitor STI571.[25] Recently, extensive studies have been performed on c-Abl in the nervous system to investigate its role in neurodegenerative disease.[9–14,26] For example, c-Abl kinase has been reported to regulate the accumulation of AIMP2 (aminoacyl tRNA synthetase complex-interacting multifunctional protein 2), FBP1 (far upstream element-binding protein 1), and α-synuclein in PD models.[9,10,11] Here, by using the SILAC analysis, we identified p38α as a major

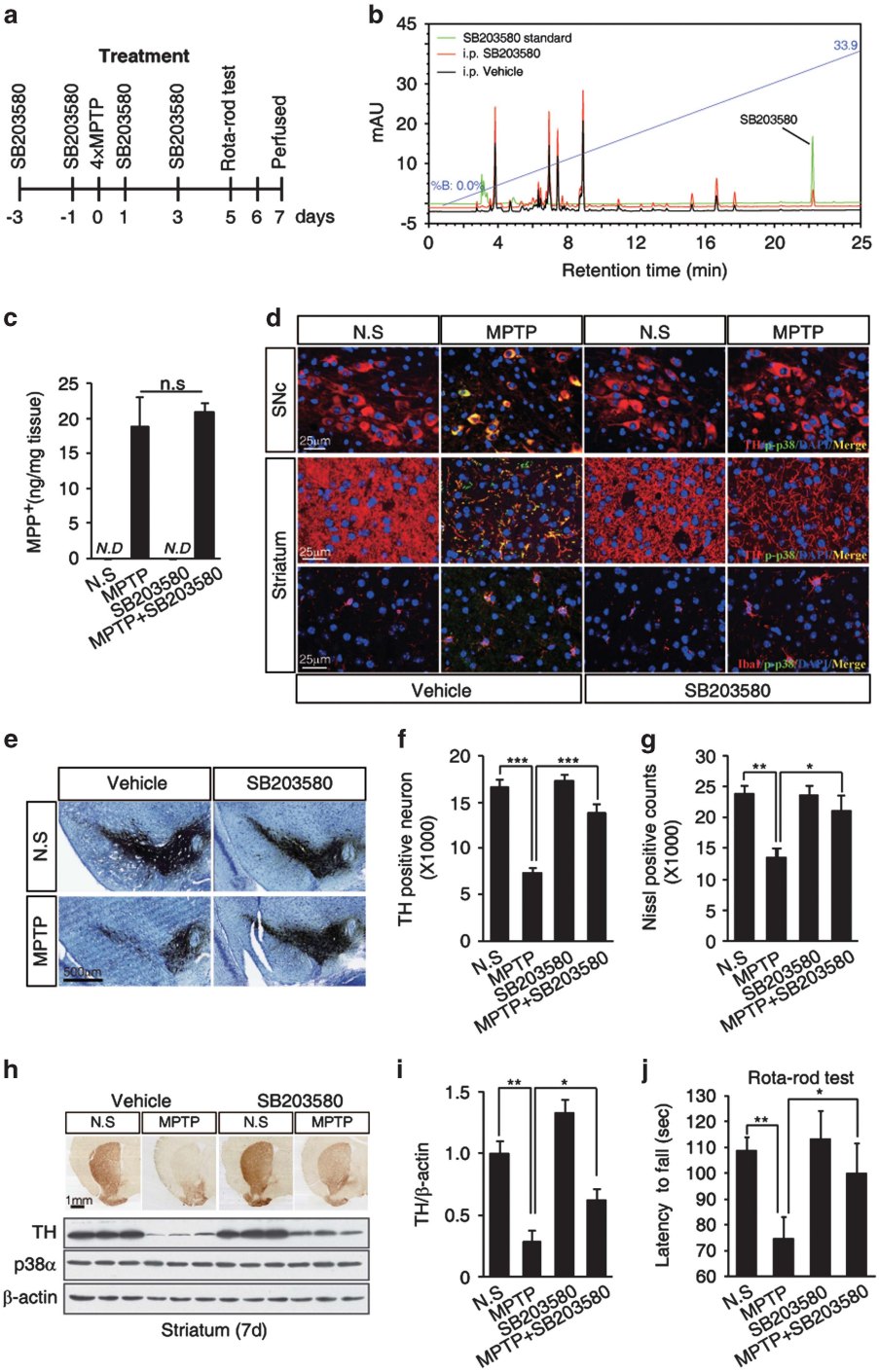

Figure 6 The p38α inhibitor SB203580 protects against MPTP-induced dopaminergic neuronal death and motor deficits. (**a**) Experimental design. C57BL/6J mice were treated with SB203580 (four i.p. injections of 5 mg/kg at 1-day intervals) followed by an additional injection 12 h after treatment with MPTP (four i.p. injections of 20 mg/kg at 2 h intervals). The mice were killed 7 days after the final MPTP injection. For behavioral testing, the mice were trained on the Rota-Rod at 10 r.p.m. for 2 days before any drug treatment. At 5 days after the final MPTP injection, behavior was tested using the Rota-Rod. (**b**) Brain penetration of SB203580 was detected by HPLC analysis in ventral midbrain after 2 h of intraperitoneal injection. (**c**) Mice were treated as in (**a**) and killed 90 min after final MPTP injection. The levels of MPP^+ in the striatum were measured. ND, not detected ($n=3$ per group). (**d**) Immunofluorescence images of TH/Iba1 (red), phospho-p38α (green), and merged staining (yellow) in substantia nigra or striatum from the MPTP alone or MPTP/SB203580-treated mice. (**e**) Photomicrographs of TH and Nissl co-stained sections in the substantia nigra of mice treated as in (**a**). (**f** and **g**) The number of TH-positive neurons (**f**) and Nissl-stained cells (**g**) was determined by stereological quantification for (**e**). The data are presented as mean ± S.E.M. (ANOVA, $^*P<0.05$, $^{***}P<0.001$, $n=5$). (**h**) Photomicrographs of TH-immunostained sections of the striatum from the mice treated as in (**a**) (upper panel). The striatal tissue lysates were immunoblotted with anti-TH antibody (bottom panel). (**i**) Normalized levels of TH protein. The data are expressed as mean ± S.E.M. (ANOVA, $^*P<0.05$, $^{**}P<0.01$, $n=3$). (**j**) The latency of the mice on the Rota-Rod. The data are expressed as mean ± S.E.M. (ANOVA, $^*P<0.05$, $^{**}P<0.01$, $n=11$–15 per group)

substrate of c-Abl in the process of oxidative stress-induced neuronal cell death.

We previously showed that c-Abl phosphorylates mammalian Ste20-like kinase 1 (MST1) and enhances MST1-mediated signaling to promote oxidative stress-induced neuronal death.[6] The kinase MST1 may act upstream of p38*α* and c-Jun N-terminal kinase (JNK) in response to oxidative stress.[27,28] In this study, we clearly demonstrated that c-Abl directly phosphorylates p38*α* and plays a critical role in the MPTP-induced pathogenesis of PD. However, the role of MST1 in c-Abl-mediated p38*α* activation requires further investigation.

The p38*α* is a subgroup of MAPKs that mediate responses to extracellular stimulation.[29] The p38*α* is typically activated by an upstream MAPK kinase such as MKK3 or MKK6.[30] The T cell antigen receptor signaling pathway bypasses the typical MAPK cascade and activates p38*α* via phosphorylation at Tyr-323 followed by autophosphorylation of p38*α* in the activation loop.[31] We demonstrated that c-Abl directly phosphorylates and activates p38*α* in response to oxidative stress to induce neuronal death. Furthermore, we showed that a p38*α* inhibitor rescued dopaminergic neurons from MPTP-induced death; thus, p38*α* may represent a therapeutic target for PD treatment.

Various inhibitors including STI571 and SB203580 have been used in the treatment of diseases outside of central nervous system because of their low brain penetration. Moreover, the therapeutic limitation of these inhibitors is caused by their specificity. Therefore, the development of high brain-permeable and target-specific inhibitors of c-Abl and p38 would facilitate the therapeutic treatment for the neurodegenerative diseases.

In summary, the present study identified p38*α* as a novel substrate of c-Abl during MPTP-induced death of dopaminergic neurons, providing further support for the crucial role of c-Abl in the development of PD. In future, it would be valuable to explore the efficacy of c-Abl–p38*α* inhibition as a therapeutic strategy for PD.

Materials and Methods

Animals. Mice were maintained under conditions of a 12-h light/dark cycle at 23 °C and were provided with food and water *ad libitum* in the Animal Care Facility at the Institute of Biophysics (Beijing, China). All experiments involving animals were approved by and conformed to the guidelines of the institutional animal care and use committee at the Institute of Biophysics of the Chinese Academy of Sciences (Beijing, China).

Generation of mice with a conditional c-Abl KO in neurons. c-Abl$^{flox/+}$ (male) and c-Abl$^{flox/+}$(female) mice were crossed to generate c-Abl$^{flox/flox}$ mice. The c-Abl$^{flox/flox}$ mice were crossed with c-Abl$^{flox/+}$; CaMKIIα-iCre$^{+/-}$ mice, and the offspring c-Abl$^{flox/flox}$; CaMKIIα-iCre$^{+/-}$ mice (c-Abl KO) and c-Abl$^{flox/flox}$ mice (WT) were used in the experiments. This approach enabled Cre recombinase to inactivate the c-Abl gene specifically in cells in which the CaMKIIα promoter is active. The floxed c-Abl gene was identified via PCR using primer-1 (5′-CAGCAACCGGCTTGCATG-3′) and primer-2 (5′- AGGCCTTCTTCCTGATAG TC-3′), yielding PCR products of 200 and 230 bp for the WT and floxed alleles, respectively. For PCR of the CaMKIIα-Cre allele, we used the forward primer 5′-GGTT CTCCGTTTGCACTCAGGA-3′ and the reverse primer 5′-CCTGTTGTTCAG CTTGCACCAG-3′, yielding a 350-bp product.

Drug treatment *in vivo*. Adult C57BL/6J mice were administered four intraperitoneal injections of 30 mg/kg STI571, 5 mg/kg SB203580, or vehicle (saline) at 1-day intervals at 12 h before and after MPTP injection (Figures 2a and 6a). The mice were administered four intraperitoneal injections of 20 mg/kg MPTP as previously described.[32] At 7 days after the final MPTP injection, the animals were killed, and the striatum was dissected and processed for western blot analysis. In some cases, the animals were perfused with 4% paraformaldehyde in 0.1 M phosphate buffer (pH 7.4), and 5 μm coronal paraffinized sections were prepared for immunohistochemistry assays.

TSA immunohistochemistry. To detect the phosphorylation of p38, tyramide signal amplification (TSA) method was performed according to the protocol from the manufacturer (PerkinElmer, Waltham, MA, USA). Coronal sections were incubated with anti-phospho-p38 (1 : 100, Cell Signaling Technology, 9216, Beverly, MA, USA) and followed by horseradish peroxidase (HRP) reaction and visualization with TSA kit. The sections were then incubated with rabbit polyclonal anti-TH (1 : 200, Pel Freez Biologicals, P40101, Rogers, AR, USA) or anti-Iba1 (1 : 100, Wako, 019-19741, Chuo-Ku, Osaka, Japan) and visualized by immunofluorescent microscopy.

Measurement of striatal MPP$^+$ levels. Mice were killed 90 min after the final MPTP injection, and striata were dissected and sonicated. After centrifugation, the supernatant was added 4 volume acetonitrile to precipitated protein. The supernatants were dehydrated and resolved in 100 μl water. Then, 50 μl of supernatant was injected into the Ultimate XB-C18 column (4.6 × 250 mm, 5 μm, Welch, Shanghai, China) and eluted with ultrapure water (1‰ trifluoroacetate)/acetonitrile (1‰ trifluoroacetate) in a gradient manner. Finally, the MPP$^+$ was detected at 280 nm.

Brain permeability analysis of STI571 and SB203580. Mice were intraperitoneally injected with STI571 (150 mg/kg) or SB203580 (50 mg/kg). After 2 h, the ventral midbrain was collected and sonicated followed by centrifugation at 14 000 r.p.m. for 15 min. Next, 4 volume acetonitrile was added into the supernatant to precipitated proteins and followed by centrifugation at 14 000 r.p.m. for 15 min. The second supernatant was dehydrated and resolved in 100 μl water. Then, 50 μl of supernatant was injected onto a Ultimate XB-C18 column (4.6 × 250 mm, 5 μm, Welch) and eluted with ultrapure water (1‰ trifluoroacetate)/acetonitrile (1‰ trifluoroacetate) in a gradient manner. Finally, STI571 was detected at 275 nm and SB203580 was detected at 300 nm.

Stereological analysis. The brains were post-fixed using 4% paraformaldehyde, cryoprotected in 30% sucrose, and processed for immunohistochemistry. Coronal sections 40 μm in thickness were sliced throughout the brain, including the substantia nigra and striatum, and every fourth section was analyzed. For TH labeling, the slices were treated with a 1 : 1000 dilution of rabbit polyclonal anti-TH (P40101, Pel Freez Biologicals) followed by biotinylated goat anti-rabbit IgG and streptavidin-conjugated HRP (Vectastain ABC kit, Vector Laboratories, Burlingame, CA, USA). Positive immunostaining was visualized using 3,3′-diaminobenzidine (DAB) followed by a reaction with hydrogen peroxide (DAB kit, Vector Laboratories). Stained sections were mounted onto slides and counterstained with Nissl (1% Toluidine Blue). The total numbers of TH-stained or Nissl-stained neurons from the substantia nigra pars compacta region were counted using the Optical Fractionator tool in Stereo Investigator software (MicroBrightfield, Williston, VT, USA).

Motor coordination test. Motor performance was estimated using an accelerating Rota-Rod (Panlab, LE8200, Energia, Cornella, Spain). After mice were placed on the rod, the timer was started. The mice were trained on the Rota-Rod at 10 r.p.m. three times per day (at 1 h intervals) for 2 days before testing. During testing, the rod accelerated from 4 to 40 r.p.m. over a period of 300 s. The mice remaining on the apparatus after 600 s were removed, and the time was recorded as 600 s. Each result represents the average endurance of three consecutive measurements performed at 1 h intervals.

Plasmids and transfection. The plasmids used were pCMV-Myc-c-Abl WT and KD as previously described.[6] The 3 × FLAG-tagged p38α constructs inserted into the pCMV10-3XFLAG expression vector were created using the mouse cDNA library. The Y182F and Y323F mutants of p38α were generated via site-directed mutagenesis. All mutations were verified via sequencing. Fragments of the GST-p38α plasmids were cloned into pGEX6P1 at the *Bam*HI and *Not*I restriction sites via PCR. Unless stated otherwise, all transfections were performed in complete

medium containing Vigofect (Vigorous Biotechnology, Beijing, China) according to the manufacturer's instructions.

SILAC labeling. 'Light', 'medium', and 'heavy' arginine (Arg0 $^{12}C_6^{14}N_4$, Arg6 $^{13}C_6^{14}N_4$, and Arg10 $^{13}C_6^{15}N_4$, respectively) and lysine (Lys0 $^{12}C_6^{14}N_2$, Lys6 $^{13}C_6^{14}N_2$, and Lys8 $^{13}C_6^{15}N_2$, respectively) and DMEM deficient in arginine and lysine were purchased from Pierce (Waltham, MA, USA). Dialyzed FBS and penicillin/streptomycin were purchased from Gibco (Waltham, MA, USA). SILAC media were prepared using 10% dialyzed FBS, 1% penicillin/streptomycin, and 50 mg/l arginine and lysine. The cells were cultured for a minimum of eight passages. The labeling efficiency was determined via LC-MS. The labeling efficiency was 100%, and <5% proline conversion was observed.

Identification of tyrosine-phosphorylated peptides. Labeled SH-SY5Y cells were seeded at 2.0×10^6 cells per 15 cm dish. When the cells reached 85% confluence, they were left untreated or were treated with 800 μM H_2O_2 for 30 min. In some groups, this treatment was preceded by a 1-h pretreatment with 5 μM STI571. The cells were harvested in 9 M urea sample buffer (9 M urea, 20 mM HEPES, pH 8, 1 mM Na_3VO_4, 2.5 mM $Na_4P_2O_7$, and 1 mM β-glycerophosphate). Then, 10 mg of protein from each group of labeled cells was mixed. The mixed cell lysates were sonicated, centrifuged, reduced, alkylated, and digested with trypsin overnight at room temperature. To ensure complete digestion before purification, the cell lysates were analyzed via SDS-PAGE electrophoresis followed by Coomassie Blue staining. The digested lysates were acidified in 1% trifluoroacetate (TFA), and the peptides were purified using C18 Sep-Pak columns (WAT051910; Waters, Milford, MA, USA). The columns were washed with 8 volumes of 0.1% TFA. Next, the peptides were eluted with 40% acetonitrile /0.1% TFA and then dried. The tyrosine-phosphorylated peptides were isolated using 40 μl of an agarose-conjugated phosphotyrosine antibody (4G10; Millipore, Billerica, MA, USA) in immunoprecipitation (IP) buffer (50 mM MOPS/NaOH, pH 7.2, 10 mM Na_2HPO_4, and 50 mM NaCl). The immunoprecipitates were washed twice with 1 ml of IP buffer and then three times with 1 ml of water. The tyrosine-phosphorylated peptides were eluted in 100 μl of 0.15% TFA at room temperature. These peptides were concentrated and purified using ZipTip Pipette Tips (ZTC18M008; Millipore) according to the manufacturer's instructions. The concentrated and purified peptides were analyzed via LC-MS using an LTQ Orbitrap XL (Thermo Scientific, Waltham, MA, USA).

Co-immunoprecipitation and immunoblotting. Cells for co-immunoprecipitation were lysed in buffer containing 50 mM HEPES, pH 7.9, 150 mM NaCl, 10% Glycerol, 1% Triton-100, 1.5 mM $MgCl_2$, 0.1 M NaF, 1 mM ethylene glycol tetraacetic acid (EGTA), 2 mM phenylmethylsulfonyl fluoride, 2 μg/ml Aprotinin and Leupeptin, and 1 mM sodium vanadate. Lysates were centrifuged at $12\,000 \times g$ for 15 min at 4 °C before immunoprecipitation and precleared with 2 μl IgG and protein G agarose beads at 4 °C for 2 h. Following the removal of the beads by centrifugation, lysates were incubated with appropriate antibodies in the presence of 30 μl of protein G agarose beads for at least 2 h at 4 °C. Tissues or cells for immunoblotting were lysed in buffer containing 50 mM HEPES, pH 7.4, 150 mM NaCl, 1% Nonidet P-40, 0.1% deoxycholate, 0.05% SDS, 0.1 M NaF, 1 mM EGTA, 2 mM phenylmethylsulfonyl fluoride, 2 μg/ml aprotinin and leupeptin, and 1 mM sodium vanadate. Protein concentration was determined using a Bio-Rad protein assay kit (Bio-Rad, Hercules, CA, USA). Proteins were separated on a 10% polyacrylamide gel and transferred to a methanol-activated PVDF membrane (GE Healthcare, Little Chalfont, Buckinghamshire, UK). The membrane was blocked for 1 h in Tris-buffered saline and Tween-20 (TBST) containing 5% milk and subsequently probed with primary antibodies overnight at 4 °C. After incubating for 1 h with goat-anti-mouse or goat-anti-rabbit HRP-conjugated secondary antibodies (GE Healthcare), protein level was detected with Super Signal West Pico and Femto Luminol reagents (Thermo Scientific). The antibodies used were anti-c-Abl (2862, Cell Signaling Technology, Cambridge, MA, USA), anti-phospho-c-Abl (2861, Cell Signaling Technology), anti-p38 (9212, Cell Signaling Technology), anti-phospho-p38 (9211, Cell Signaling Technology), anti-TH (2792, Cell Signaling Technology), anti-phospho-tyrosine (4G10, Millipore), anti-Myc (MBL, Woburn, MA, USA), anti-FLAG (Sigma, St. Louis, MO, USA), anti-GFP (Invitrogen, Waltham, MA, USA), anti-β-actin (60008-1-Ig, Proteintech Group, Campbell Park, Chicago, IL, USA), and anti-GAPDH (CW0266A, CWBiotech, Beijing, China).

***In vitro* kinase assay.** Recombinant active c-Abl kinase (Millipore, Billerica, MA, USA) was incubated in 20 mM Tris, pH 7.5, 10 mM $MgCl_2$, 100 μM ATP, and 1 μg of the substrate GST-p38α. After incubation at room temperature for 30 min, the kinase reaction products were separated via SDS-PAGE and analyzed via immunoblotting using the indicated antibodies.

Statistical analysis. The intensity of the western blot bands was determined using ImageJ software (NIH, Bethesda, MD, USA). Statistical analyses were performed via one-way analysis of variance (ANOVA) followed by Tukey's *post hoc* test or via a two-tailed Student's *t*-test. The data are presented as mean $\pm$ S.E.M. $^*P < 0.05$, $^{**}P < 0.01$, and $^{***}P < 0.001$ denote the significance thresholds.

Conflict of Interest

The authors declare no conflict of interest.

Acknowledgements. We thank Dr. Yong Cang for the c-Abl$^{flox/flox}$ mice and Dr. Xiang Yu for the CamKIIα-iCre mice. We thank Dr. Peng Xue and Dr. Fuquan Yang for the mass-spec technical help. We thank Dr. Lili Niu for the HPLC technical help. We also thank the members of the Yuan laboratory for critical reading of the manuscript and helpful discussion. This work was supported by the National Science Foundation of China (Grant Nos. 81125010 and 81030025), the National Basic Research Program of China (973-2011CB504105 to ML, 973-2012CB910701 and 2013DFA31990 to ZY), and Cross-disciplinary Collaborative Teams Program for Science, Technology and Innovation (2014–2016) from Chinese Academy of Sciences.

1. Savitt JM, Dawson VL, Dawson TM. Diagnosis and treatment of Parkinson disease: molecules to medicine. *J Clin Invest* 2006; **116**: 1744–1754.
2. Gasser T. Molecular pathogenesis of Parkinson disease: insights from genetic studies. *Exp Rev Mol Med* 2009; **11**: e22.
3. Dauer W, Przedborski S. Parkinson's disease: mechanisms and models. *Neuron* 2003; **39**: 889–909.
4. Langston JW, Ballard P, Tetrud JW, Irwin I. Chronic Parkinsonism in humans due to a product of meperidine-analog synthesis. *Science* 1983; **219**: 979–980.
5. Sirvent A, Benistant C, Roche S. Cytoplasmic signalling by the c-Abl tyrosine kinase in normal and cancer cells. *Biol Cell* 2008; **100**: 617–631.
6. Xiao L, Chen D, Hu P, Wu J, Liu W, Zhao Y *et al.* The c-Abl-MST1 signaling pathway mediates oxidative stress-induced neuronal cell death. *J Neurosci* 2011; **31**: 9611–9619.
7. Liu W, Wu J, Xiao L, Bai Y, Qu A, Zheng Z *et al.* Regulation of neuronal cell death by c-Abl-Hippo/MST2 signaling pathway. *PLoS One* 2012; **7**: e36562.
8. Cancino GI, Perez de Arce K, Castro PU, Toledo EM, von Bernhardi R, Alvarez AR. c-Abl tyrosine kinase modulates tau pathology and Cdk5 phosphorylation in AD transgenic mice. *Neurobiol Aging* 2011; **32**: 1249–1261.
9. Ko HS, Lee Y, Shin JH, Karuppagounder SS, Gadad BS, Koleske AJ *et al.* Phosphorylation by the c-Abl protein tyrosine kinase inhibits parkin's ubiquitination and protective function. *Proc Natl Acad Sci USA* 2010; **107**: 16691–16696.
10. Imam SZ, Zhou Q, Yamamoto A, Valente AJ, Ali SF, Bains M *et al.* Novel regulation of parkin function through c-Abl-mediated tyrosine phosphorylation: implications for Parkinson's disease. *J Neurosci* 2011; **31**: 157–163.
11. Mahul-Mellier AL, Fauvet B, Gysbers A, Dikiy I, Oueslati A, Georgeon S *et al.* c-Abl phosphorylates alpha-synuclein and regulates its degradation: implication for alpha-synuclein clearance and contribution to the pathogenesis of Parkinson's disease. *Hum Mol Genet* 2014; **23**: 2858–2879.
12. Hebron ML, Lonskaya I, Moussa CE. Nilotinib reverses loss of dopamine neurons and improves motor behavior via autophagic degradation of alpha-synuclein in Parkinson's disease models. *Hum Mol Genet* 2013; **22**: 3315–3328.
13. Imam SZ, Trickler W, Kimura S, Binienda ZK, Paule MG, Slikker W Jr *et al.* Neuroprotective efficacy of a new brain-penetrating C-Abl inhibitor in a murine Parkinson's disease model. *PLoS One* 2013; **8**: e65129.
14. Karuppagounder SS, Brahmachari S, Lee Y, Dawson VL, Dawson TM, Ko HS. The c-Abl inhibitor, nilotinib, protects dopaminergic neurons in a preclinical animal model of Parkinson's disease. *Sci Rep* 2014; **4**: 4874.
15. Dai H, Marbach P, Lemaire M, Hayes M, Elmquist WF. Distribution of STI-571 to the brain is limited by P-glycoprotein-mediated efflux. *J Pharmacol Exp Ther* 2003; **304**: 1085–1092.
16. Mahul-Mellier AL, Fauvet B, Gysbers A, Dikiy I, Oueslati A, Georgeon S *et al.* c-Abl phosphorylates alpha-syn and regulates its degradation, implication for alpha-syn clearance and contribution to the pathogenesis of Parkinson's Disease. *Hum Mol Genet* 2014; **23**: 2858–2879.
17. Cao C, Leng Y, Li C, Kufe D. Functional interaction between the c-Abl and Arg protein-tyrosine kinases in the oxidative stress response. *J Biol Chem* 2003; **278**: 12961–12967.

18. Gotoh A, Miyazawa K, Ohyashiki K, Tauchi T, Boswell HS, Broxmeyer HE *et al.* Tyrosine phosphorylation and activation of focal adhesion kinase (p125FAK) by BCR-ABL oncoprotein. *Exp Hematol* 1995; **23**: 1153–1159.
19. Sanguinetti AR, Mastick CC. c-Abl is required for oxidative stress-induced phosphorylation of caveolin-1 on tyrosine 14. *Cell Signal* 2003; **15**: 289–298.
20. Burton EA, Oliver TN, Pendergast AM. Abl kinases regulate actin comet tail elongation via an N-WASP-dependent pathway. *Mol Cell Biol* 2005; **25**: 8834–8843.
21. Rothweiler U, Aberg E, Johnson KA, Hansen TE, Jorgensen JB, Engh RA. p38alpha MAP kinase dimers with swapped activation segments and a novel catalytic loop conformation. *J Mol Biol* 2011; **411**: 474–485.
22. Casanova E, Fehsenfeld S, Mantamadiotis T, Lemberger T, Greiner E, Stewart AF *et al.* A CamKIIalpha iCre BAC allows brain-specific gene inactivation. *Genesis* 2001; **31**: 37–42.
23. Kohutnicka M, Lewandowska E, Kurkowska-Jastrzebska I, Czlonkowski A, Czlonkowska A. Microglial and astrocytic involvement in a murine model of Parkinson's disease induced by 1-methyl-4-phenyl-1,2,3,6-tetrahydropyridine (MPTP). *Immunopharmacology* 1998; **39**: 167–180.
24. Hantschel O, Superti-Furga G. Regulation of the c-Abl and Bcr-Abl tyrosine kinases. *Nat Rev Mol Cell Biol* 2004; **5**: 33–44.
25. Marley SB, Deininger MW, Davidson RJ, Goldman JM, Gordon MY. The tyrosine kinase inhibitor STI571, like interferon-alpha, preferentially reduces the capacity for amplification of granulocyte-macrophage progenitors from patients with chronic myeloid leukemia. *Exp Hematol* 2000; **28**: 551–557.
26. Schlatterer SD, Acker CM, Davies P. c-Abl in neurodegenerative disease. *J Mol Neurosci* 2011; **45**: 445–452.
27. Johnston AM, Naselli G, Gonez LJ, Martin RM, Harrison LC, DeAizpurua HJ. SPAK, a STE20/SPS1-related kinase that activates the p38 pathway. *Oncogene* 2000; **19**: 4290–4297.
28. Bi W, Xiao L, Jia Y, Wu J, Xie Q, Ren J *et al.* c-Jun N-terminal kinase enhances MST1-mediated pro-apoptotic signaling through phosphorylation at serine 82. *J Biol Chem* 2010; **285**: 6259–6264.
29. Zarubin T, Han J. Activation and signaling of the p38 MAP kinase pathway. *Cell Res* 2005; **15**: 11–18.
30. Enslen H, Raingeaud J, Davis RJ. Selective activation of p38 mitogen-activated protein (MAP) kinase isoforms by the MAP kinase kinases MKK3 and MKK6. *J Biol Chem* 1998; **273**: 1741–1748.
31. Mittelstadt PR, Yamaguchi H, Appella E, Ashwell JD. T cell receptor-mediated activation of p38{alpha} by mono-phosphorylation of the activation loop results in altered substrate specificity. *J Biol Chem* 2009; **284**: 15469–15474.
32. Jackson-Lewis V, Przedborski S. Protocol for the MPTP mouse model of Parkinson's disease. *Nat Protoc* 2007; **2**: 141–151.